



Testing the capability of spectral resolution of the new multispectral sensors on detecting the severity of grey leaf spot disease in maize crop

Inos Dhau, Elhadi Adam, Onisimo Mutanga, Kwabena Ayisi, Elfatih Mohamed Abdel-Rahman, John Odindi & Mhosisi Masocha

To cite this article: Inos Dhau, Elhadi Adam, Onisimo Mutanga, Kwabena Ayisi, Elfatih Mohamed Abdel-Rahman, John Odindi & Mhosisi Masocha (2018) Testing the capability of spectral resolution of the new multispectral sensors on detecting the severity of grey leaf spot disease in maize crop, Geocarto International, 33:11, 1223-1236, DOI: [10.1080/10106049.2017.1343391](https://doi.org/10.1080/10106049.2017.1343391)

To link to this article: <https://doi.org/10.1080/10106049.2017.1343391>



Accepted author version posted online: 16 Jun 2017.

Published online: 30 Jun 2017.



Submit your article to this journal [↗](#)



Article views: 212



View Crossmark data [↗](#)



Citing articles: 1 View citing articles [↗](#)



Testing the capability of spectral resolution of the new multispectral sensors on detecting the severity of grey leaf spot disease in maize crop

Inos Dhau^a, Elhadi Adam^b, Onesimo Mutanga^c, Kwabena Ayisi^d, Elfatih Mohamed Abdel-Rahman^e, John Odindi^e and Mhosisi Masocha^f

^aGeography and Environmental Studies, University of Limpopo, Sovenga, South Africa; ^bSchool of Geography, Archaeology and Environmental Studies, University of Witwatersrand, Johannesburg, South Africa; ^cDepartment of Geography, University of Kwa-Zulu Natal, Pietermaritzburg, South Africa; ^dRisk and Vulnerability Science Centre / VLIR-IUC Programme, University of Limpopo, Sovenga, South Africa; ^eGeography, University of Kwazulu-Natal, Pietermaritzburg, South Africa; ^fGeography and Environmental Science, University of Zimbabwe, Harare, Zimbabwe

ABSTRACT

In this study, we tested whether GLS field symptoms on maize can be detected using hyperspectral data re-sampled to WorldView-2, Quickbird, RapidEye and Sentinel-2 resolutions. To achieve this objective, Random Forest algorithm was used to classify the 2013 re-sampled spectra to represent the three identified disease severity categories. Results showed that Sentinel-2, with 13 spectral bands, achieved the highest overall accuracy and kappa value of 84% and 0.76, respectively, while the WorldView-2, with eight spectral bands, yielded the second highest overall accuracy and kappa value of 82% and 0.73, respectively. Results also showed that the 705 and 710 nm red edge bands were the most valuable in detecting the GLS for Sentinel-2 and RapidEye, respectively. On the re-sampled WorldView 2 and Quickbird sensor resolutions, the respective 608 and 660 nm in the yellow and red bands were identified as the most valuable for discriminating all categories of infection.

ARTICLE HISTORY

Received 2 November 2016
Accepted 31 May 2017

KEYWORDS

Field spectroscopy; grey leaf spot; spectral re-sampling; multispectral remote sensing

1. Introduction

Maize is the most important cereal crop in sub-Saharan Africa (SSA) and contributes 15–50% of energy in human diets in the region (Archetti et al. 2009; Kagoda et al. 2011). The current annually per capita consumption of maize is estimated to be about 112 kg, which is equivalent to 308 g per day per capita (Degraeve et al. 2016). Annual demand for maize in the region is projected to increase at a rate of 2.4% per annum up to 2025 (Pinstrup-Andersen et al. 1999). Currently, household and per capita maize consumption in the SSA region is highest among developing countries (Pingali and Pandey 2001), consequently measures to improve maize production are considered essential for food security in the region (Watkins and Von Braun 2003). Whereas studies in SSA have shown that there is an increase in total maize production over years (Beyene and Kassie 2015), most of this increase has been attributed to area expansion rather than optimization of production techniques and therefore increased yield on existing acreage (Beyene and Kassie 2015). Beyene and Kassie (2015) attribute the low yield in the region to the slow adoption of precision agriculture and associated technologies.

In the SSA, an interplay of biotic and abiotic factors is known to cause up to 80% maize yield losses (DeVries and Toenniessen 2001; Pingali and Pandey 2001). Among the major diseases that threaten the stability of maize production in the region, particularly South Africa, are grey leaf spot (GLS) (Derera et al. 2008), Northern Corn Leaf Blight (Welz and Geiger 2000; Degefu et al. 2004) and *Phaeosphaeria* leaf spot (Sibiya et al. 2011).

The GLS caused by *Cercospora zeaе-maydis* was first identified from specimens collected in 1924 by Tehon and Daniels in Alexander County in southern Illinois near the Mississippi River (Ward et al. 1999). In South Africa, GLS was first noted in KwaZulu-Natal province in 1988 and has since spread rapidly to neighbouring provinces and other Southern Africa countries (Ward et al. 1997). More recently, molecular techniques have allowed a detailed analysis of the genetic variability of the pathogen population and the existence of two very distinct groups has been revealed (Meisel et al. 2009). A review of the literature suggests that there are two possible species complexes associated with GLS, namely the *C. sorghi* complex (*C. sorghi* and *C. sorghi* var. *maydis*) and the *C. zeaе-maydis* complex (Groups I and II). The description of *C. zeina* has now resolved some of this taxonomic uncertainty by demonstrating that Group II is in fact a distinct species (*C. zeina*) and that Group I to which the name *C. zeaе-maydis* applies apparently does not occur in South Africa (Dunkle and Levy 2000; Crous et al. 2006; Meisel et al. 2009).

GLS is currently recognized as one of the most maize damaging diseases in the region, especially in areas with warm temperatures and prolonged relative humidity (Ward et al. 1999; Wegary et al. 2003; Paul and Munkvold 2005; Derera et al. 2008; Meisel et al. 2009; Lyimo et al. 2012).

Recently, a number of countries, e.g. Kenya, Zimbabwe and South Africa, have reported 30–60% maize yield losses due to GLS, hence a serious threat to food security (Ward et al. 1997; Muriithi and Gathama 1998). The disease reduces maize yield by damaging photosynthetic tissue and increasing stem and root lodging (Derera et al. 2008).

In maize, the GLS symptoms first appear on the lower leaves as small tan spots typically long rectangular or irregular 1–3 mm shapes (Ward et al. 1999). At the early stage, immature GLS lesions are not easily distinguishable from lesions caused by other foliar maize pathogens (Ward et al. 1999). However, mature foliar lesions symptomatic of GLS can readily be distinguished from other maize foliar diseases; grey to tan rectangular shape (5–70 mm long by 2–4 mm wide) running parallel to the leaf veins (Ward et al. 1999). The latent period for GLS is long compared to other foliar pathogens and can take as long as 14–28 days after infection for lesions to sporulate (Beckman and Payne 1982). Under severe epidemics, lesions may coalesce and blight the entire leaves (Beckman and Payne 1982; Ward et al. 1999).

An integrated approach to planning and management of GLS in maize is critical for sustainable production and improvement in yield quality and quantity. This approach requires, *inter alia* that maize disease information is available in ways that allow for timely adoption of relevant management practice at the right place (de Bie 2000; Pingali and Pandey 2001; Geerts et al. 2006; Mulla 2013). A basic principle of precision agriculture is that the presence, distribution and intensity of a specific stress factor within a field must be identifiable (Hillnhütter et al. 2011). The distinctive patchy appearance on maize canopy due to GLS infestation makes the disease suitable for the adoption of precision agriculture tools such as geo-information and remote sensing techniques (Hillnhütter et al. 2011).

Visual field-based observation has been used to determine GLS severity and incidences (Elwinger et al. 1990; Bubeck et al. 1993; Nilsson 1995; Munkvold et al. 2001); however, such visual protocols are often expensive, time-consuming and prone to human error. The assessment of disease severity and its real-time field distribution could be valuable for the adoption and timing of relevant mitigation measures like fungicide applications. Since the GLS is a foliar fungal disease, and plant leaves have a well-known spectral signature, remote sensing technologies can be used to complement field-based protocol in determining infection onset and severity (Nutter and Schultz 1995).

The use of remote sensing in plant pathology and crop protection is well established (Jackson 1986; Hatfield and Pinter 1993; Nilsson 1995; West et al. 2003; Bock et al. 2010; Mahlein et al. 2012). For example, field spectroscopy has been used to detect maize dwarf mosaic viral disease (Ausmus and

Hilty 1973), wheat yellow rust (Bravo et al. 2003; Moshou et al. 2004), and bacterial leaf blight in rice (Yang 2010). Several studies have described the views of sensing leaf reflectance in the visible (VIS, 400–700 nm), near infrared (NIR, 700–1000 nm) and short-wave infrared (SWIR, 1000–2500 nm) for detecting changes in plant vitality with emphasis on fungal plant diseases using non-imaging spectroradiometers (Steddom et al. 2005; Delalieux et al. 2007; Mahlein et al. 2010; Rumpf et al. 2010). Whereas field spectroscopy has proved to be useful in disease detection, up-scaling the developed models to the current available spaceborne or airborne sensors remains a common challenge. This is due to the fact that most of the current operational satellites lack the necessary fine spectral resolution sensors, and hence, the application of satellite remote sensing for crop disease detection is still in its infancy.

Recently, some researchers have suggested that this limitation could be overcome by re-sampling field spectral data to band settings of existing sensors. For mapping relevance, this can be followed by testing their capability in existing coarser spectral resolution formats for different remote sensing applications, where hyperspectral data are not available (Slaton et al. 2001; Crawford et al. 2003; Cho and Skidmore 2009). Indeed, several studies (Mutanga and Skidmore 2005; Adam et al. 2012; Mansour et al. 2012; Petropoulos et al. 2012) have re-sampled field spectra data to band settings of existing or planned sensors to broaden their remote sensing applications. Whereas these studies have been able to demonstrate the possibility to up-scale field spectra to airborne or satellite sensors, a major challenge of such up-scaling remains the field spectrometer's higher signal-to-noise ratio than satellite or airborne images, due to the former's shorter signal path length (Milton et al. 2009). Nevertheless, Mutanga et al. (2015) recently provided an insight into the magnitude of errors expected when up-scaling field spectral models to airborne or satellite image. They note that the minor difference between the model developed on the re-sampled field spectra in comparison to the actual image indicates the relevance of field spectroscopy and spectral re-sampling in mapping (Mutanga et al. 2015).

The advent of new multispectral sensors such as RapidEye, Sentinel-2 and WorldView-2 series is seen as a trade-off between benefits offered by multispectral and hyperspectral remotely sensed data. This is mainly due to their fine spatial resolution and reasonable number of spectral bands, which are configured within unique portions of the electromagnetic spectrum such as the red edge. These new sensors provide an opportunity for more crop monitoring and precision agriculture.

In this study, we sought to determine whether field spectrometry measurements re-sampled to different multispectral sensor resolutions can be used to detect the severity of GLS infection in maize. The specific objectives were the following: (i) to test if severity of GLS can be detected by hyperspectral data re-sampled to Sentinel-2, WorldView-2, RapidEye and Quickbird sensor resolutions and (ii) to determine the best spectral bands that are important for detecting GLS. Reliable results from the study offer an opportunity for mapping and monitoring GLS infestations in maize crop using sensors on aerial and satellite platforms.

2. Material and methods

2.1. Identification of GLS stages

This study was carried out at Cedara Agricultural Research Farm, located at 1076 metres above sea level and approximately 100 km in-land of South Africa's major port city of Durban in KwaZulu-Natal province (30°16 East, 29°32 South). GLS symptoms were carefully identified in the field over two seasons in March 2013 and 2014 for spectral data acquisition. In specific, GLS symptoms and severity were visually assessed using an expert knowledge approach (Elwinger et al. 1990; Bubeck et al. 1993; Munkvold et al. 2001; Bock et al. 2010; Sibiyi et al. 2011). GLS severity was assessed by estimating per cent maize leaf area affected by the disease. The severity of the disease on the maize leaves was then rated using a modified scale of 0–5 as described by (Paul and Munkvold 2004). The six scales were 0 (no disease), 1 (10–20% leaf area affected by the disease), 2 (21–40% leaf area affected by the disease); 3 (41–60% leaf area affected by the disease), 4 (61–80% leaf area affected by the disease) and 5 (81–100% leaf area affected by the disease). Further, we followed a recommendation by Nutter

et al. (1991) that leaves with less than 20% GLS affected area were considered to be in an early stage of infection (herein is considered as healthy leaves), while leaves with 21–60% GLS affected area were considered to be in the moderate stage of infection. Leaves with 61–100% were considered to be severely infected (Figure 1).

2.2. Field spectral measurements and processing

Maize leaf spectral measurements from the three GLS infection stages; viz healthy, moderate and severe were collected using Analytical Spectral Devices (ASD) FieldSpec³ optical sensor (ASD, Inc., Boulder, CO, USA). Leaf spectra were taken under clear sunny and cloud-free sky from 10:00 to 14:00 local time (GMT + 2). The ASD FieldSpec³ spectrometer has a 350–2500 nm spectral range with 1.4 and 2 nm sampling intervals for the ultraviolet to visible near infrared region (350–1000 nm) and the short-wave infrared region (1000–2500 nm), respectively.

The plant and leaf samples representing each of the GLS infection stages were randomly chosen and six measurements per leaf were acquired. The six measurements were then averaged to derive the representative reflectance spectra for the leaf. A white reference spectral measurement on the calibration panel was performed every 10–20 measurements to offset any change in the atmospheric condition and sun irradiance spectrum. Field spectral measurements were done over two (2013 and 2014) growing seasons. The 2013 field spectra were used for training the random forest (RF) classifier model, while the 2014 field spectra were used to test the stability and the accuracy of the RF classification model. The sample size for each GLS infection stage is shown in Figure 1.

The visual GLS severity assessment was benchmarked by displaying narrowband normalised difference vegetation index (NDVI) boxplots of the three severity stages (i.e. healthy, moderate and severe) during the two seasons (Figure 2). The NDVIs were calculated using field spectrometric hyperspectral measurements. Figure 2 reveals that the spread of NDVIs during the two seasons was nearly the same.

The reflectance spectra from the three GLS infection stages (Figure 3) were then re-sampled to the Sentinel-2, WorldView-2, Quickbird and RapidEye spectral resolutions using a Gaussian model in ENVI 4.7 image processing software (ENVI 2009). The method uses a Gaussian model with a full width at half maximum (FWHM) equal to the band centres provided (Table 1). The re-sampled spectra were then used for the further analysis.

2.3. RF classifier and accuracy assessment

The RF algorithm was used to classify the re-sampled spectra to represent the three identified disease severity categories. RF is an ensemble learning technique developed by Breiman (2001) to improve the classification and regression of trees by combining a large set of decision trees. RF grows multiple unpruned trees (*n*tree) on bootstrap samples of the original data. Each tree is grown on a bootstrap sample (2/3 of the original data known as ‘in-bag’ data) taken with replacement from the original data (Breiman 2001). The samples not in the bootstrap sample are referred to as the out-of-bag (OOB) sample. The OOB sample (~37% of the total data) can be used to estimate the misclassification error and variable importance. Trees are split to many nodes using random subsets of variables (*m*try); the default *m*try value is the square root of the total number of variables. From the *m*try selected variables, the variable that yields the highest decrease in impurity is chosen to split the samples at each node (Breiman 2001). A tree is grown to its maximum size without pruning until the nodes are pure. This means that the nodes hold samples of the same class or contain certain number of samples. A prediction of the response variable (e.g. GLS stages) is made by aggregating the prediction over all trees. In a classification experiment, a majority vote from all the trees in the ensemble determines the final prediction (Breiman 2001). A more detailed description of RF can be found in among others Breiman (2001).

RF also provides variable importance measurement, which is a measure of the contribution of each variable (band) in the final predictive model. This is a metric of how much classification accuracy


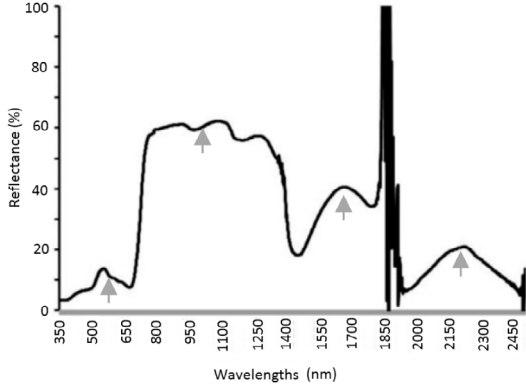

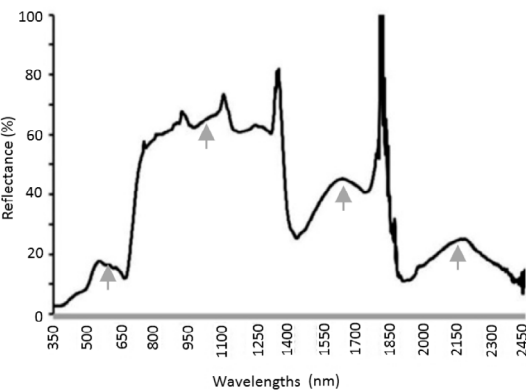

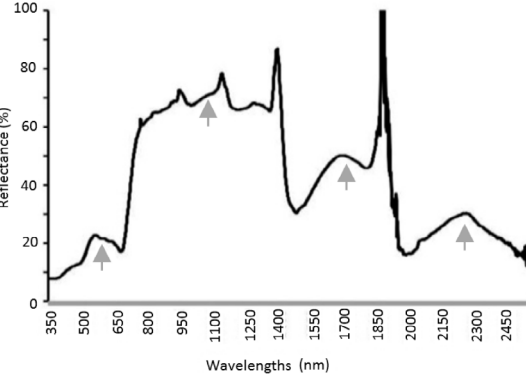
Disease status	Mean Reflectance	Training samples (2013)	Testing samples (2014)
<p>Healthy</p> 		88	68
<p>Moderate</p> 		92	70
<p>Severe</p> 		86	75

Figure 1. Maize grey leaf spot (GLS) infection stages (healthy, moderate and severe) and their mean reflectance spectra. The reflectance spectra were collected under field conditions using Analytical Spectral Devices (ASD) FieldSpec® 3 optical sensor during 2013 and 2014 growing seasons. The arrows show the spectral regions where major differences between the three disease stages are observed.

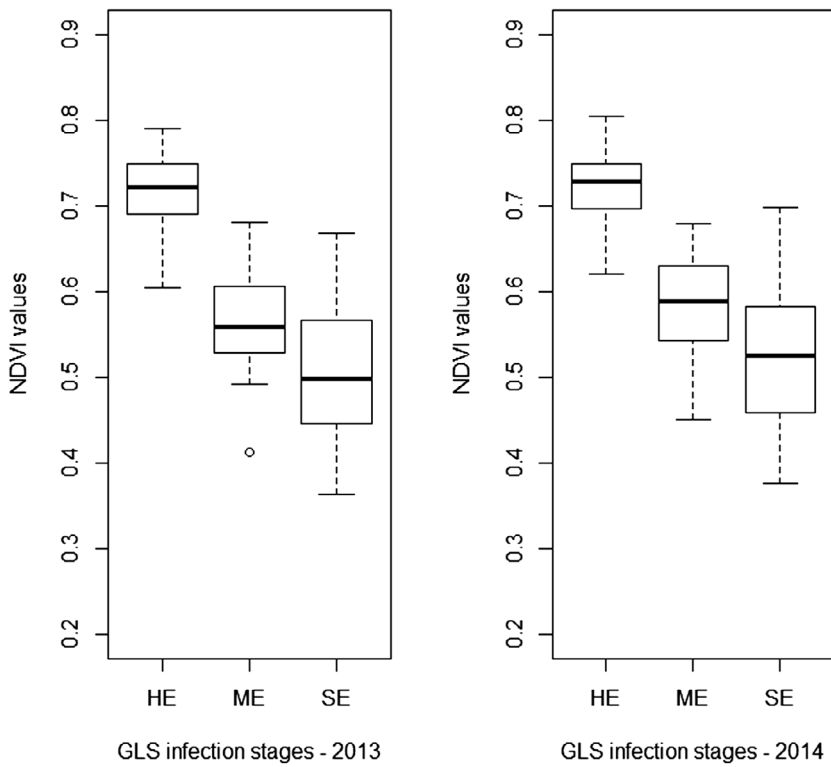


Figure 2. Boxplots showing the median, quartile and the spread of narrowband normalized difference vegetation index (NDVI) for healthy (H), moderate (M) and severely (S) grey leaf spot infected maize leaves during two growing seasons (March 2013 and March 2014). NDVIs were calculated from field spectrometric hyperspectral measurements.

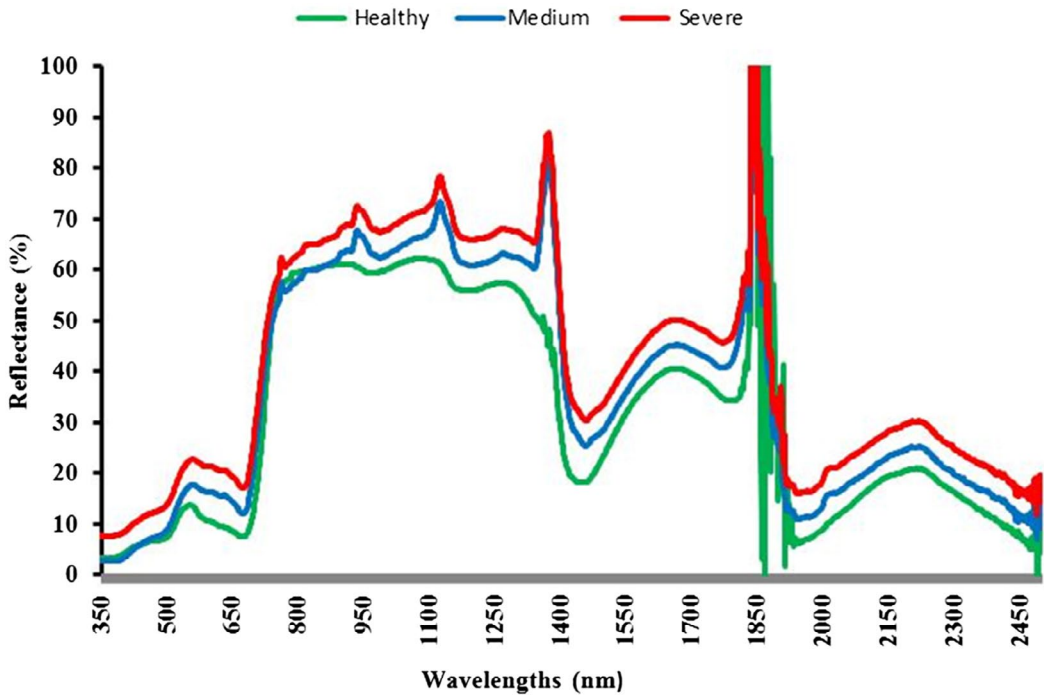


Figure 3. Comparison between the mean reflectance of the three maize GLS infection stages (healthy, moderate and severely).

Table 1. Multispectral sensors and their spectral properties.

Sensor	Band description	Band centre (nm)	bandwidth (nm)
Sentinel-2	B1	443	20
	B2	490	65
	B3	560	35
	B4	665	30
	B5	705	15
	B6	740	15
	B7	783	20
	B8	842	115
	B8b	865	20
	B9	945	20
	B10	1380	30
	B11	1610	90
WorldView-2	B12	2190	120
	Coastal	427	50
	Blue	478	60
	Green	546	70
	Yellow	608	40
	Red	659	60
	Red-edge	725	40
	NIR-1	831	125
Quickbird	NIR-2	908	180
	Blue	485	70
	Green	560	80
	Red	660	60
RapidEye	NIR	830	140
	Blue	475	70
	Green	555	70
	Red	658	55
	Red-edge	710	40
	NIR	805	90

would decrease if data of a particular variable (band) were removed while all variables remained the same (Breiman 2001; Verikas et al. 2011).

In this study, we used this variable importance measurement to determine the importance of each band from the different sensors in detecting GLS infection. The choice of the RF algorithm was motivated by its superiority over competing statistical methods such as discriminant analysis, canonical variate analysis, classification trees, support vector machines and principal component analysis (Cochrane 2000; Mutanga and Skidmore 2004; Adam and Mutanga 2009) for vegetation monitoring. However, the superiority of a classification method is highly dependent on the type and features of the data under investigation.

In RF, only two parameters (i.e. *mtry* and *ntree*) have to be optimized. The default number of trees (*ntree*) is usually 500, while the default value for the number of variables (*mtry*) is \sqrt{p} where P equals the number of predictor variables within a data-set. In this study a grid-search approach based on the OOB estimate of error was used to find the optimal combination for these two parameters (*ntree* and *mtry*) (Adam et al. 2014). The grid-search value for *mtry* was varied from 1 to the total number of bands for each sensor with a single value interval, while the range of the grid search value for the *ntree* parameter was varied from 500 (default value) to 10,000 with an interval of 500 (20 steps). For example, the grid search yielded a total of 160 and 80 combinations of *ntree* and *mtry* values for WorldView-2 and Quickbird, respectively. The data-set collected in 2013 was used to optimize and train RF model.

We used the 2013 data-set to train the RF model; while the 2014 data-set was used to assess the model accuracy (sample size for both 2013 and 2014 data-sets is shown in Figure 1). A confusion matrix was constructed to compute the overall accuracy (OA), user's accuracy (UA) and producer's accuracy (PA) as criteria for evaluating the generalization ability (accuracy) of the RF classifiers. OA is a ratio (%) between the number of correctly classified samples and the number of test samples, while UA represents the likelihood that a sample belongs to specific class and the classifier accurately

assigns it to such a class. PA expresses the probability of a certain class being correctly classified. Kappa statistic that uses the K statistic was also calculated to determine if one error matrix is significantly different from another. The kappa coefficient provides a measure of the actual agreement between reference data and a random classifier. If the kappa coefficients are equal or close to one, then there is perfect agreement.

3. Results

3.1. Optimizing RF parameters

Results from the grid search indicated that OOB error rate is sensitive to *ntree* and *mtry* parameters. Different combinations of *ntree* and *mtry* produced the lowest OOB error rates for the different sensors. The default settings for both *ntree* and *mtry* did not produce better results for the different sensors. For example, the combination of *mtry* value of 4 and *ntree* value of 500 produced lowest OOB error for Quickbird, while the combination of *mtry* value of 10 with different *ntree* values (3000, 4500 and 9500) produced the lowest OOB error (0.08) for Sentinel-2 (Figure 4). The highest OOB error rates (0.13–0.16%) were produced with lowest *mtry* values across different sensors (Figure 4).

3.2. Classification results

The classification accuracies obtained using field spectra re-sampled to WorldView-2, Quickbird, RapidEye and Sentinel 2 sensor resolutions for both training and testing data-sets are shown in Table 2. RF produced the highest OA (84.04%) and kappa value of 0.76 for Sentinel-2. On the other

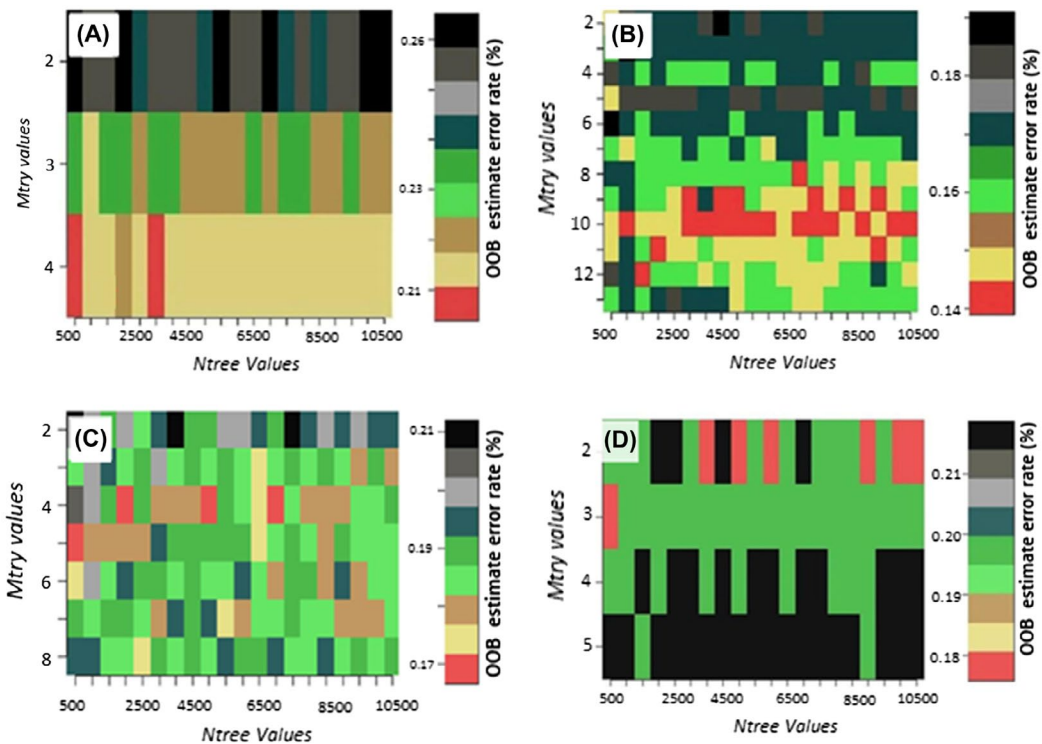


Figure 4. Optimization of the random forest parameters (*mtry* and *ntree*) using the grid search procedure. The OOB method was used to determine the error rates for the different combinations; 60 combinations for Quickbird (A), 240 combination for Sentinel-2 (B), 160 combinations for WorldView-2 (C) and 80 combinations for RapidEye (D).

Table 2. Random forest classification overall accuracy (OA) and Kappa coefficient for detecting maize grey leaf spot disease using ground-based hyperspectral data and resampled multispectral data (simulated to four sensors spectral resolutions). The classification model was trained on the 2013 data and its accuracy was assessed using the independent 2014 test data.

	Sensor	Testing data	
		OA	KAPPA
Hyperspectral			
	FieldSpec ³ spectroradiometer	89.2	0.83
Multispectral			
	Worldview-2	82.16	0.73
	Quickbird	76.77	0.66
	RapidEye	81.22	0.72
	Sentinel-2	84.04	0.76

Table 3. Classification confusion matrix of random forest (RF) classifier for detection the three studied maize grey leaf spot (GLS) infection stages (H: healthy, M: moderate and S: severe) using the resampled Sentinel-2 bands for the 2014 data set.

Class	2014 test data			Total
	H	M	S	
H	59	6	3	68
M	2	64	4	70
S	5	14	56	75
Total	66	84	63	213

Notes: Overall accuracy (%) = 84.04; Producer's accuracy (%) = 89.39; User's accuracy (%) = 86.76; Kappa = 0.76.

hand, the lowest OA (76.77%) was achieved when Quickbird was used. It is also worth noting that the difference between the results of training data-set and the test data-set for all sensors is about $\pm 2\%$, which can be considered insignificant.

Results on Table 3 provide further details about the confusion matrix, PA and UA accuracies achieved for Sentinel-2, the multispectral sensor with the highest accuracy.

3.3. Measuring the importance of multispectral variables (bands) in detecting maize GLS stages in maize

Figure 5 shows the most important bands in each sensor for detecting GLS in maize leaves. The importance of each band was measured using mean decrease in accuracy in RF algorithm (Figure 5). The most important bands are located at different electromagnetic positions for each sensor. For example, the red edge (705 nm) was found to be the most important (highest mean decrease in accuracy) band for Sentinel-2. Using the WorldView-2, the yellow band located at 608 nm was the most important. The most important band for detecting the GLS using Quickbird was the red (660 nm), while red (658 nm) and the red edge bands (710 nm) were the most important bands when RapidEye was used (Figure 5).

4. Discussion

The GLS is considered one of the most serious diseases affecting maize production in many countries, particularly in North America and Africa. Timely detection and control of GLS requires intensive spatial data collection for designing optimal mitigation strategies (Mulla 2013). A number of studies have demonstrated the importance of remote sensing data in defining the spatial variability of pests and diseases in crops (Zhang et al. 2003; Qin and Zhang 2005; Falkenberg et al. 2007; Yang 2012). The main objective of this study was to test the use of the spectral resolution of the newly developed multispectral sensors in detecting the severity of GLS in maize. Results indicate that different stages of GLS can be reliably discriminated using the newly developed multispectral sensors such as WorldView-2, Sentinel-2 and RapidEye.

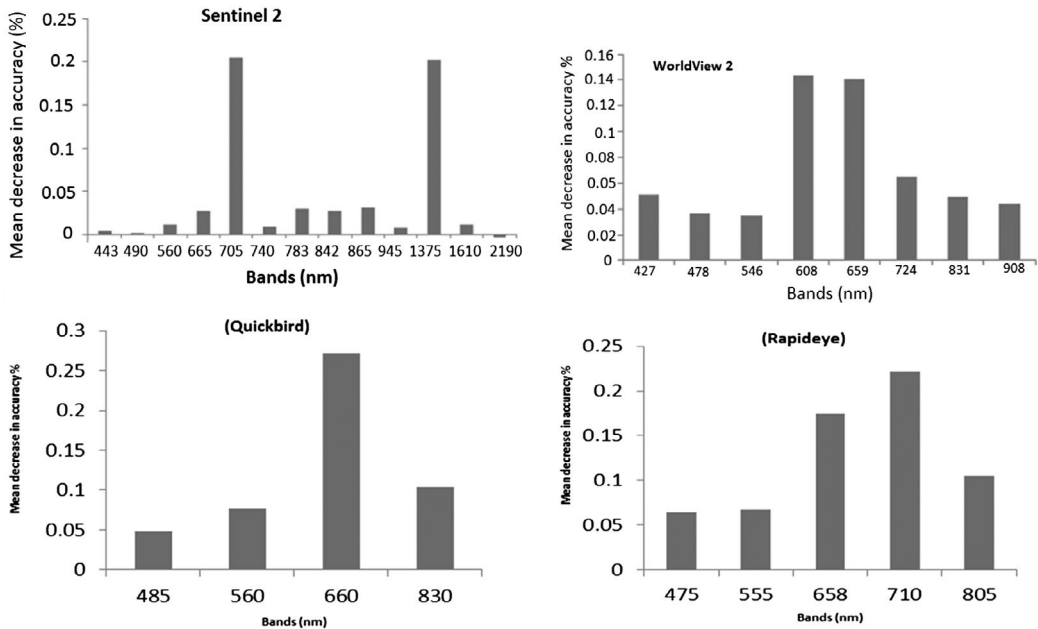


Figure 5. The importance of each band for different sensors used in this study for distinguishing the three maize GLS infection stages using random forest (RF).

The spectral and spatial resolutions of the newly developed multispectral sensors offer significant potential in real-time data provision, necessary for precision agriculture. The newly developed multispectral sensors can be considered a compromise between multispectral and hyperspectral sensor limitations, useful for the adoption of improved agricultural management practices. Hyperspectral remotely sensed data are costly and difficult to process. However, it provides the ability to investigate spectral response of different vegetation stresses in narrow spectral bands (10 nm wide) within a wide spectral range, which is otherwise masked by relatively cheap, broad and limited bands inherent in existing multispectral sensors.

Results in this study suggest that the new generation Sentinel-2's 705 nm red edge band, the WorldView-2's 608 nm yellow band, the Quickbird's 660 nm red and RapidEye's 710 nm red edge bands are all suitable for detecting GLS disease. However, the re-sampled Sentinel-2 data-set can discriminate healthy from GLS-infected leaves with highest OA (84%) and a Kappa value over 0.76. Results in this study also suggest that the WorldView-2 is valuable for detecting GLS under field conditions (OA of 82% and Kappa of 0.73).

These results demonstrate for the first time that the Sentinel-2 wavebands are strategically positioned for agricultural applications, suitable for discriminating healthy from GLS-infested maize as well as different levels of infestation. Conversely, the OA achieved in this study suggests that existing multispectral sensors such as QuickBird, RapidEye and WorldView-2, in comparison to Sentinel-2, are less optimally positioned and therefore less suited for detecting GLS infestation. Overall, our results highlight the value of multispectral image data in detecting and mapping plant diseases.

Although the Sentinel-2 achieved the highest accuracy, due to its high spectral resolution (13 bands), its spatial resolution (10 m) is coarser than the WorldView-2 (2 m). Thus, WorldView-2 provides a viable up-scaling option for mapping GLS, as it is characterized by a higher spatial resolution and an acceptable level of classification accuracy achieved with less bands than Sentinel-2.

Our results concur with findings from literature (Moshou et al. 2004, Yang et al 2005, Graeff et al 2006). For instance, Moshou et al. (2004) reported that the reflectance at 680, 725 and 750 nm could

be used to detect yellow rust in winter wheat while (Yang et al. 2005) established that the band centred at 694 nm can be used to detect green bug infestation. (Graeff et al. 2006) successfully distinguished powdery mildew infested from healthy wheat leaves with reflectance at 490, 510, 516, 540, 780 and 1300 nm during early infestation.

The high accuracy achieved in this study contributes towards the development of operational remote sensing systems on advanced multispectral sensors. This approach is valuable for mapping crop diseases, particularly in Africa where high cost of hyperspectral image data-sets has impeded wide adoption of remotely sensed imagery. These findings may be useful in assessing the spectral configurations of new sensors under development and inform spectral adjustments and optimization for specific applications on the up-scaled image data (Mutanga et al. 2005; Adjorlolo et al. 2012).

5. Conclusions

This paper aimed at discriminating GLS severity in maize using field spectrometry data re-sampled to different multispectral sensor resolutions.

The results demonstrate that:

- (1) Field symptoms of GLS in maize can be detected using hyperspectral field spectra re-sampled to different multispectral sensor resolutions.
- (2) Using RF algorithm, Sentinel-2 and WorldView-2 have a higher and acceptable accuracy level, respectively, in discriminating different maize GLS stages using the red, red edge and SWIR regions of the spectrum.

Overall, our results open up opportunities for discriminating GLS in maize using multispectral sensors such as Sentinel-2 and WorldView-2. We however recommend that more studies should be pursued to investigate the feasibility of using multispectral sensors and their spatial resolutions to detect and map the spatial distribution of maize GLS severity. The use of new generation multispectral sensors offer a great opportunity for detection and mapping of GLS from space, offering real-time operational data, ultimately improving strategies for mitigating crop damage and yield loss.

Acknowledgements

We would like to thank Prof John Derera (African Centre for Crop Improvement, University of KwaZulu-Natal) for his assistance during the field data collection and identifying the disease stages.

Disclosure statement

No potential conflict of interest was reported by the authors.

References

- Adam E, Mutanga O. 2009. Spectral discrimination of papyrus vegetation (*Cyperus papyrus* L.) in swamp wetlands using field spectrometry. *ISPRS J Photogramm Remote Sens.* 64:612–620.
- Adam E, Mutanga O, Odindi J, Abdel-Rahman EM. 2014. Land-use/cover classification in a heterogeneous coastal landscape using RapidEye imagery: evaluating the performance of random forest and support vector machines classifiers. *Int J Remote Sens.* 35:3440–3458.
- Adam EM, Mutanga O, Rugege D, Ismail R. 2012. Discriminating the papyrus vegetation (*Cyperus papyrus* L.) and its co-existent species using random forest and hyperspectral data resampled to HYMAP. *Int J Remote Sens.* 33(Jan 20):552–569.
- Adjorlolo C, Mutanga O, Cho M, Ismail R. 2012. Challenges and opportunities in the use of remote sensing for C 3 and C 4 grass species discrimination and mapping. *Afr J Range Forage Sci.* 29:47–61.
- Archetti M, Döring TF, Hagen SB, Hughes NM, Leather SR, Lee DW, Lev-Yadun S, Manetas Y, Ougham HJ, Schaberg PG. 2009. Unravelling the evolution of autumn colours: an interdisciplinary approach. *Trends Ecol Evol.* 24:166–173.

- Ausmus BS, Hilty JW. 1973. Reflectance studies of healthy, maize dwarf mosaic virus-infected, and *Helminthosporium maydis* infected corn leaves. *Remote Sens Environ.* 2:77–81.
- Beckman PM, Payne GA. 1982. External growth, penetration, and development of *Cercospora zeae-maydis* in corn leaves. *Phytopathology.* 72:810–815.
- Beyene AD, Kassie M. 2015. Speed of adoption of improved maize varieties in Tanzania: an application of duration analysis. *Technol Forecasting Soc Change.* 96(96):298–307.
- de Bie CAJM. 2000. Comparative performance of agro-ecosystems [PhD]. Wageningen: Wageningen University.
- Bock C, Poole G, Parker P, Gottwald T. 2010. Plant disease severity estimated visually, by digital photography and image analysis, and by hyperspectral imaging. *Crit Rev Plant Sci.* 29:59–107.
- Bravo C, Moshou D, West J, McCartney A, Ramon H. 2003. Early disease detection in wheat fields using spectral reflectance. *Biosyst Eng.* 84:137–145.
- Breiman L. 2001. Random forests. *Mach Learn.* 45:5–32.
- Bubeck D, Goodman M, Beavis W, Grant D. 1993. Quantitative trait loci controlling resistance to gray leaf spot in maize. *Crop Sci.* 33:838–847.
- Cho M, Skidmore A. 2009. Hyperspectral predictors for monitoring biomass production in mediterranean mountain grasslands: majella national park, Italy. *Int J Remote Sens.* 30:499–515.
- Cochrane M. 2000. Using vegetation reflectance variability for species level classification of hyperspectral data. *Int J Remote Sens.* 21:2075–2087.
- Crawford MM, Ham J, Chen Y, Ghosh J. 2003. Random forests of binary hierarchical classifiers for analysis of hyperspectral data. Proceedings of the Advances in Techniques for Analysis of Remotely Sensed Data, 2003 IEEE Workshop on; IEEE.
- Crous PW, Groenewald JZ, Groenewald M, Caldwell P, Braun U, Harrington TC. 2006. Species of *Cercospora* associated with grey leaf spot of maize. *Stud Mycol.* 55:189–197.
- Degefu Y, Lohtander K, Paulin L. 2004. Expression patterns and phylogenetic analysis of two xylanase genes (htxyl1 and htlyl2) from *Helminthosporium turcicum*, the cause of northern leaf blight of maize. *Biochimie* 86:83–90.
- Degraeve S, Madege RR, Audenaert K, Kamala A, Ortiz J, Kimanya M, Tiisekwa B, De Meulenaer B, Haesaert G. 2016. Impact of local pre-harvest management practices in maize on the occurrence of *Fusarium* species and associated mycotoxins in two agro-ecosystems in Tanzania. *Food Control* 59:225–233.
- Delalieux S, Van Aardt J, Keulemans W, Schrevens E, Coppin P. 2007. Detection of biotic stress (*Venturia inaequalis*) in apple trees using hyperspectral data: non-parametric statistical approaches and physiological implications. *Eur J Agron.* 27:130–143.
- Derera J, Tongoona P, Pixley KV, Vivek B, Laing MD, van Rij NC. 2008. Gene action controlling gray leaf spot resistance in Southern African maize germplasm. *Crop Sci.* 48:93–98.
- DeVries J, Toenniessen GH. 2001. Securing the harvest: biotechnology, breeding, and seed systems for African crops. Wallingford: CABI.
- Dunkle LD, Levy M. 2000. Genetic relatedness of African and United States populations of *Cercospora zeae-maydis*. *Phytopathology.* 90:486–490.
- Elwinger G, Johnson M, Hill R, Ayers J. 1990. Inheritance of resistance to gray leaf spot of corn. *Crop Sci.* 30:350–358.
- ENVI. 2009. ENVI 47: environment for visualizing images Exelis Visual Information Solutions. CO: ITT Industries.
- Falkenberg NR, Piccinni G, Cothren JT, Leskovar DI, Rush CM. 2007. Remote sensing of biotic and abiotic stress for irrigation management of cotton. *Agric Water Manage.* 87:23–31.
- Geerts S, Raes D, Garcia M, Castillo CD, Buytaert W. 2006. Agro-climatic suitability mapping for crop production in the Bolivian Altiplano: a case study for quinoa. *Agric Forest Meteorol.* 139:399–412.
- Graeff S, Link J, Claupein W. 2006. Identification of powdery mildew (*Erysiphe graminis* sp. tritici) and take-all disease (*Gaeumannomyces graminis* sp. tritici) in wheat (*Triticum aestivum* L.) by means of leaf reflectance measurements. *Cent Eur J Biol.* 1:275–288.
- Hatfield P, Pinter P. 1993. Remote sensing for crop protection. *Crop Prot.* 12:403–413.
- Hillnhütter C, Mahlein AK, Sikora RA, Oerke EC. 2011. Remote sensing to detect plant stress induced by *Heterodera schachtii* and *Rhizoctonia solani* in sugar beet fields. *Field Crops Res.* 122:70–77.
- Jackson RD. 1986. Remote sensing of biotic and abiotic plant stress. *Annu Rev Phytopathol.* 24:265–287.
- Kagoda F, Derera J, Tongoona P, Coyne DL, Talwana HL. 2011. Grain yield and heterosis of maize hybrids under nematode infested and nematicide treated conditions. *J nematol.* 43:209.
- Lyimo HJE, Pratt RC, Mnyuku RSOW. 2012. Composted cattle and poultry manures provide excellent fertility and improved management of gray leaf spot in maize. *Field Crops Res.* 126:97–103.
- Mahlein A-K, Oerke E-C, Steiner U, Dehne H-W. 2012. Recent advances in sensing plant diseases for precision crop protection. *Eur J Plant Pathol.* 133:197–209.
- Mahlein A-K, Steiner U, Dehne H-W, Oerke E-C. 2010. Spectral signatures of sugar beet leaves for the detection and differentiation of diseases. *Precis Agric.* 11:413–431.
- Mansour K, Mutanga O, Everson T, Adam E. 2012. Discriminating indicator grass species for rangeland degradation assessment using hyperspectral data resampled to AISA Eagle resolution. *ISPRS J Photogramm Remote Sens.* 70:56–65.

- Meisel B, Korsman J, Kloppers FJ, Berger DK. 2009. *Cercospora zeina* is the causal agent of grey leaf spot disease of maize in southern Africa. *Eur J Plant Pathol.* 124:577–583.
- Milton E, Schaepman M, Anderson K, Kneubühler M, Fox N. 2009. Progress in field spectroscopy. *Remote Sens Environ.* 113:S92–S109.
- Moshou D, Bravo C, West J, Wahlen S, McCartney A, Ramon H. 2004. Automatic detection of ‘yellow rust’ in wheat using reflectance measurements and neural networks. *Comput Electron Agric.* 44:173–188.
- Mulla DJ. 2013. Twenty five years of remote sensing in precision agriculture: key advances and remaining knowledge gaps. *Biosyst Eng.* 358–371.
- Munkvold G, Martinson C, Shriver J, Dixon P. 2001. Probabilities for profitable fungicide use against gray leaf spot in hybrid maize. *Phytopathology.* 91:477–484.
- Muriithi L, Gathama S. 1998. Gray leaf spot of maize: a new disease on increase. *Crop Prot Newsl.*
- Mutanga O, Adam E, Adjorlolo C, Abdel-Rahman EM. 2015. Evaluating the robustness of models developed from field spectral data in predicting African grass foliar nitrogen concentration using WorldView-2 image as an independent test dataset. *Intern J Appl Earth Obs Geoinf.* 34(34):178–187.
- Mutanga O, Skidmore A. 2004. Integrating imaging spectroscopy and neural networks to map grass quality in the kruger national park, South Africa. *Remote Sens Environ.* 90:104–115.
- Mutanga O, Skidmore A. 2005. Discriminating tropical grass canopies grown under different nitrogen treatments using spectra resampled to HYMAP. *Intern J Geoinformatics.* 1:21–32.
- Mutanga O, Skidmore A, Kumar L, Ferwerda J. 2005. Estimating tropical pasture quality at canopy level using band depth analysis with continuum removal in the visible domain. *Intern J Remote Sens.* 26:1093–1108.
- Nilsson H-E. 1995. Remote sensing and image analysis in plant pathology. *Can J Plant Pathol.* 17:154–166.
- Nutter Jr FW, Schultz PM. 1991. Improving the accuracy and precision of disease assessments: selection of methods and use of computer-aided training programs. *Can J Plant Pathol.* 17:174–184.
- Nutter FW Jr, Schultz PM. 1995. Improving the accuracy and precision of disease assessments: selection of methods and use of computer-aided training programs. *Can J Plant Pathol.* 17:174–184.
- Paul PA, Munkvold G. 2004. A model-based approach to preplanting risk assessment for gray leaf spot of maize. *Phytopathology.* 94:1350–1357.
- Paul P, Munkvold G. 2005. Influence of temperature and relative humidity on sporulation of *Cercospora zae-maydis* and expansion of gray leaf spot lesions on maize leaves. *Plant Dis.* 89:624–630.
- Petropoulos GP, Kalaitzidis C, Prasad Vadrevu K. 2012. Support vector machines and object-based classification for obtaining land-use/cover cartography from Hyperion hyperspectral imagery. *Comput Geosci.* 41:99–107.
- Pingali P, Pandey S. 2001. World maize needs meeting: technological opportunities and priorities for the public sector. In: En Pingali PL, editor. CIMMYT 1999–2000 world maize facts and trends meeting world maize needs: technological opportunities and priorities for the public sector. Mexico: CIMMYT. Part 1; p. 1–20.
- Pinstrup-Andersen P, Pandya-Lorch R, Rosegrant MW. 1999. World food prospects: critical issues for the early twenty-first century. Washington, DC: International Food Policy Research Institute.
- Qin Z, Zhang M. 2005. Detection of rice sheath blight for in-season disease management using multispectral remote sensing. *Intern J App Earth Obs Geoinf.* 7:115–128.
- Rumpf T, Mahlein A-K, Steiner U, Oerke E-C, Dehne H-W, Plümer L. 2010. Early detection and classification of plant diseases with support vector machines based on hyperspectral reflectance. *Comp Electron Agric.* 74:91–99.
- Sibiya J, Tongoona P, Derera J, van Rij N, Makanda I. 2011. Combining ability analysis for *Phaeosphaeria* leaf spot resistance and grain yield in tropical advanced maize inbred lines. *Field Crops Res.* 120:86–93.
- Slaton MR, Hunt ER, Smith WK. 2001. Estimating near-infrared leaf reflectance from leaf structural characteristics. *Am J Bot.* 88:278–284.
- Steddom K, Bredehoeft M, Khan M, Rush C. 2005. Comparison of visual and multispectral radiometric disease evaluations of *Cercospora* leaf spot of sugar beet. *Plant Dis.* 89:153–158.
- Verikas A, Gelzinis A, Bacauskiene M. 2011. Mining data with random forests: a survey and results of new tests. *Pattern Recognit.* 44:330–349.
- Ward JMJ, Laing MD, Nowell DC. 1997b. Chemical control of maize grey leaf spot. *Crop Prot.* 16:265–271.
- Ward JMJ, Stromberg EL, Nowell DC, Nutter FW Jr. 1999. Gray leaf spot: a disease of global importance in maize production. *Plant Dis.* 83:884–895.
- Watkins K, Von Braun J. 2003. Time to stop dumping on the world’s poor. *Trade Policies Food Secur.* 1–18.
- Wegary D, Habtamu Z, Singh H, Husien T. 2003. Inheritance of grey leaf spot resistance in selected maize inbred lines. *Afr Plant Prot.* 9:53–54.
- Welz H, Geiger H. 2000. Genes for resistance to northern corn leaf blight in diverse maize populations. *Plant Breeding* 119:1–14.
- West JS, Bravo C, Oberti R, Lemaire D, Moshou D, McCartney HA. 2003. The potential of optical canopy measurement for targeted control of field crop diseases. *Ann Rev Phytopathol.* 41:593–614.
- Yang C-M. 2010. Assessment of the severity of bacterial leaf blight in rice using canopy hyperspectral reflectance. *Precis Agric.* 11:61–81.

- Yang C. 2012. A high-resolution airborne four-camera imaging system for agricultural remote sensing. *Comp Electron Agric.* 88:13–24.
- Yang Z, Rao M, Elliott N, Kindler S, Popham T. 2005. Using ground-based multispectral radiometry to detect stress in wheat caused by greenbug (Homoptera: Aphididae) infestation. *Comp Electron Agric.* 47:121–135.
- Zhang M, Qin Z, Liu X, Ustin SL. 2003. Detection of stress in tomatoes induced by late blight disease in California, USA, using hyperspectral remote sensing. *Int J App Earth Obs Geoinf.* 4:295–310.